Published in final edited form as:
Mol Cancer Res. 2012 August ; 10(8): 1065–1076. doi:10.1158/1541-7786.MCR-11-0387.

Glycogen Synthase Kinase-3 promotes cell survival, growth and PAX3 levels in human melanoma cells

Jennifer D. Kubic[1], **Joseph B. Mascarenhas**[1], **Takumi Iizuka**[1], **Don Wolfgeher**[2], and **Deborah Lang**[1]

[1]Department of Medicine, University of Chicago, Chicago, IL, USA

[2]Proteomics Core Laboratory, University of Chicago, Chicago, IL, USA

Abstract

Glycogen Synthase Kinase-3 (GSK-3) is a serine/threonine kinase involved in a diverse range of cellular processes. GSK-3 exists in two isoforms, GSK-3α and GSK-3β, which possess some functional redundancy but also play distinct roles depending on developmental and cellular context. In this report we found that GSK-3 actively promoted cell growth and survival in melanoma cells, and blocking this activity with small molecule inhibitor SB216763 or gene-specific siRNA decreased proliferation, increased apoptosis and altered cellular morphology. These alterations coincided with loss of PAX3, a transcription factor implicated in proliferation, survival and migration of developing melanoblasts. We further found that PAX3 directly interacted with and was phosphorylated *in vitro* on a number of residues by GSK-3β. In melanoma cells, direct inhibition of PAX3 lead to cellular changes that paralleled the response to GSK-3 inhibition. Maintenance of PAX3 expression protected melanoma cells from the anti-tumor effects of SB216763. These data support a model wherein GSK-3 regulates proliferation and morphology of melanoma through phosphorylation and increased levels of PAX3.

Keywords

Glycogen; Synthase; Kinase-3/melanoma/PAX3

Introduction

Glycogen Synthase Kinase-3 (GSK-3) is an ubiquitously expressed, constitutively active serine/threonine kinase with demonstrated roles in a wide variety of cellular processes including metabolism, proliferation, transcriptional regulation, development and oncogenesis (1–4). GSK-3 exists in two isoforms encoded by different genes, *GSK-3*α and *GSK-3*β, which share 98% identity throughout the kinase domain but differ in the N- and C-terminal domains (2). GSK-3α or GSK-3β activity can be attenuated by phosphorylation at Ser21 or Ser9, respectively, thereby blocking GSK-3 activity for some but not all substrates (5–7). While these isoforms share functional complementarities in certain contexts, they also play distinct roles as evidenced by differing expression levels in a wide variety of tissues (2–4, 8). *Gsk-3*α and *Gsk-3*β null mice further highlight these different functions, since loss of either gene results in very different phenotypes (9–12).

Corresponding Author: Deborah Lang, PhD, University of Chicago, 5841 S. Maryland Ave., MC 5067, Chicago, IL, USA. Tel.: 773-702-6005; Fax: 773-702-8398, dlang@medicine.bsd.uchicago.edu.

The authors declare no conflict of interest.

Deregulation of GSK-3 expression and activity is implicated in the growth and survival of melanoma, but the role of the individual isoforms is less clear: the role of GSK-3α is unknown and there is limited information on GSK-3β function in melanoma. GSK-3β has been shown to protect melanoma cells from apoptosis and inhibition of GSK-3β deters mouse melanoma cell growth both *in-vitro* and *in-vivo* and parallels essential functions found in developing melanocytes (13–16).

Like GSK-3, the transcription factor PAX3 is involved in both melanocyte development and melanoma. PAX3 is expressed in melanocyte precursors and drives lineage specificity by regulating the expression of genes critical for melanogenesis (17, 18). Loss of PAX3 expression in the mouse embryo results in significant reduction in both proliferation and the number of melanoblasts (19). Due to its role in growth and survival of melanoblasts, it is not surprising that PAX3 is also expressed in melanoma (20, 21). In melanoma, PAX3 activates downstream genes implicated in melanoma proliferation, survival and metastasis such as the receptor MET (20, 22–24). How PAX3 protein is regulated in melanoma is unknown, but post-translational modification of PAX3 in other cell types alters activity and stability thereby regulating differentiation and has been implicated in tumor development (25–29). Although the mechanism of action by PAX3 in melanoma is poorly understood, its regulatory functions towards cell proliferation and differentiation in the melanoblast may be paralleled in melanoma cells by promoting cell division and resistance to apoptosis.

In this report, we found that GSK-3 acted as a critical control point of melanoma cell growth, survival, and morphology. A mechanism for GSK-dependent cell growth and morphological changes is through the regulation of PAX3 levels. Although both GSK-3α and GSK-3β are phosphorylated at Ser21 or 9, respectively, inhibition of these kinases in melanoma cells significantly reduced growth, induced apoptosis and caused dendritic process extension, mimicking differentiated melanocytes. We demonstrated that GSK-3 inhibition was correlated with a loss of PAX3 and that PAX3 loss coincided with these growth and morphological changes. GSK-3β interacted with and phosphorylated PAX3, which was correlated with PAX3 levels in melanoma cells. GSK-3α and GSK-3β partially compensated for the loss of the other in regard to proliferation and PAX3 stability. Knockout of PAX3 mimics the cell growth and length phenotypes seen upon GSK-3 inhibition and PAX3 over-expression rescued these phenotypes, suggesting GSK-3 may modulate these effects through PAX3 levels. Overall, these results demonstrate that GSK-3 and PAX3 are components of a putative pathway promoting cell proliferation, survival, and the resistance to differentiation necessary for melanoma cell survival.

Materials and Methods

Cell culture

Human melanoma lines (SKMEL-23, SKMEL-28, 537, 624, 888, and A375) (ATCC) were cultured in DMEM/10% FBS (Sigma). Melanoma cell identity was verified by morphology, growth curve analysis, and melanoma-marker testing. All cells were negative for the presence of mycoplasma. Cells at 30% confluency were supplemented with 0–20μM GSK-3 inhibitor SB216763 (Sigma) dissolved in DMSO as a carrier. The treatments were replaced daily.

RNA interference

537 and SKMEL-23 cells were transfected with siRNA against *PAX3*, *GSK-3*α, and/or *GSK-3*β, or siScramble (100 pmol; Dharmacon) using Lipofectamine-2000 (Invitrogen), following manufacturer's protocols. Four siRNAs against each of *GSK-3*α and *GSK-3*β were tested for specificity against each isoform without affecting protein levels of the other

isoform (Supplementary Fig. S1A–B). Four si*PAX3* oligos were also evaluated for efficacy (Supplemenatry Fig. S1C–D). Cell lysates were collected 72 hours post-siRNA transfection.

Western blots

Cells were lysed in RIPA buffer and 50μg total protein was separated on 4–12% Bis-Tris gels (Invitrogen), transferred to nitrocellulose membranes (Bio-Rad) then probed with 1:1000 Pax3 (University of Iowa Hybridoma Bank), 1:3000 GSK-3β, 1:1000 GSK-3α, 1:1000 phospho-GSK-3α (S21) and 1:3000 phospho-GSK-3β (S9) (Cell Signaling Technology), 1:1000 β-catenin and 1:1000 PARP (Santa Cruz), 1:1000 HA (Roche), or 1:1,000,000 vinculin antibody (Sigma). Control lysates for determination of GSK-3 phosphorylation status were treated with calf intestinal phosphatase (New England BioLabs) at 0.5units/μg of total protein at 37°C for 1 hour.

In-vitro immunoprecipitation

PAX3 and GSK-3β L-[^{35}S]-methionine-incorporated proteins were created using the TNT coupled reticulocyte lysate system (Promega) utilizing pcDNA3-PAX3-HA (18) and pcDNA3-GSK-3β (Addgene plasmid 14753, (30)) and immunoprecipitated as described (31).

Plasmid construction

The pGex2T-PAX3PD and pGex2T-PAX3PDHD-WT constructs were kindly provided by Jonathan Epstein (University of Pennsylvania). pGex2T-PAX3PDHD-ΔSERAS with the consensus motif deleted was obtained by site directed mutagenesis of pGex2T-PAX3PDHD-WT using primers 5'-TGACTCTGAAATCGATTTACCGCTGAAGAGG-3' and 5'-ACTGAGACTTTAGCTAAATGGCGACTTCTCC-3' followed by ClaI digestion removing D189–P211.

Kinase assay

GST-proteins were created and purified as described (22). Glutathione Sepharose-4B beads (GE Healthcare Biosciences) containing the GST-tagged proteins were incubated with ATP cocktail mix (25mM MOPS pH7.2, 12.5mM β-glycerol phosphate, 25mM $MgCl_2$, 5mM EGTA, 2mM EDTA, 0.25mM DTT, and 0.25mM ATP) and ATP [γ-P^{32}] with or without 60μM GSK-3β (Sigma).

Statistical analysis

Significance of the differences between variable conditions was determined by Graphpad Prism statistical software (version 5.0 Graphpad Software) utilizing the Student's t-test and Chi-square analysis with a confidence interval of 95%. All values stated as significant have p values of less than or equal to 0.005 unless indicated.

Tandem mass spectrometry (LC-MS/MS)

The pGex2T-PAX3PDHD-WT protein was phosphorylated with purified GSK-3β as described and eluted with GST elution buffer (40mM reduced glutathione in 50mM Tris-HCl, pH9.0). Phosphorylated pGex2T-PAX3PDHD-WT was purified from the eluate using the PhosphoProtein Purification Kit (Qiagen), then run on a Tris-Acetate Gel (Invitrogen) for band submission for mass spectrometry (supplementary materials). Mass spectrometry data were submitted to the Proteome Commons Tranche repository (https://www.proteomecommons.org) and assigned identifier hash: vKmrlpnOR90/JZyJT0IJN5/qDRuJIslLbP6luS9dGnH465SudjSIlSWJTrMggzaayK0zYq5GhaErBbXHYVfbWYHqWsEAAAAAAAAB0A==.

Exogenous PAX3 expression

SKMEL-23 and 537 cells were transfected with empty expression vector pcDNA3, pcDNA3-PAX3-HA, or a mock transfection using Effectene (Qiagen) according to manufacturer's protocols. Cells containing pcDNA3 or pcDNA3-PAX3-HA were selected with 2.5mg/ml Geneticin(R) (Invitrogen) in DMEM/10% FBS. After selection, cells were left untreated, treated with carrier (DMSO), or with SB216763 for 72 hours.

Results

GSK-3 inhibition blocks human melanoma cell population expansion

To determine the status of GSK-3 in human melanoma cells, 6 cell lines were analyzed for the presence and phosphorylation status of GSK-3α and GSK-3β (Fig. 1A). All cell lines expressed varying levels of both proteins. Ser21 of GSK-3α was phosphorylated in 5 lines, although 2 have low levels. Ser9 of GSK-3β was phosphorylated in all 6 lines. GSK-3 activity was determined by treating cells with DMSO or the highly specific GSK-3 small molecule inhibitor SB216763 (Fig. 1B). SB216763 renders GSK-3 inactive through ATP competition (32). β-catenin, a known phosphorylation target of GSK-3β, is stabilized upon GSK-3 inhibition. In all cell lines tested, treatment with SB216763 resulted in a higher amount of β-catenin present compared to carrier-treated cells, suggesting that GSK-3 is active in melanoma cells. To test if GSK-3 activity promotes melanoma cell growth, melanoma cells from 6 different lines were counted over time in the absence or presence of increasing concentrations of SB216763 (Fig. 2A–F). While control cells grew at similar rates, there was a minimal increase in cell numbers in cells treated with 5–20μM (SKMEL-23, 537), 10–20μM (624, 888), or 20μM SB216763 (A375). The melanoma cell lines SKMEL-28, in contrast, had no response to SB216763.

Although SB216763 is highly specific to both isoforms of GSK-3, off-target effects cannot be completely ruled out. Utilizing a complementary method, SKMEL-23 and 537 cell lines were transfected with a siRNA control (siScramble) or siRNA targeted to *GSK-3*α, *GSK-3*β, or both. Blocking expression of both isoforms replicated the cellular growth consequences of SB216763, resulting in fewer cells after 72 hours compared to controls; 48.63%+/−10.15% for SKMEL-23 and 46.26%+/−9.43% in 537 cells (Fig. 2G–H). Inhibition of only one *GSK-3* isoform also impacted cell number, although to a somewhat lesser extent of blocking both kinases in 537 cells. Inhibition of SKMEL-23 *GSK-3*α and *GSK-3*β resulted in 58.22%+/−14.21% and 41.78%+/−18.25% of the total population in comparison to control, while 537 cells had a 73.82%+/−11.83% and 72.64%+/−16.03% of the total population, respectively.

The lack of expansion of the cell population is partly due to cell cycle arrest. Flow cytometric analysis of DNA content in SKMEL-23 and 537 cells suggest a G_2/M cell cycle block (Supplementary Fig. S2). These data indicate that GSK-3 inhibition causes a substantial population reduction in melanoma cell lines and that GSK-3 isoforms are active in melanoma cells since specific knockdown results in altered phenotypes.

GSK-3 inhibition leads to apoptosis in melanoma cells

During GSK-3 inhibition the SKMEL-23 cells demonstrated apoptotic phenotypes at higher drug concentrations compared to untreated cells (Fig. 3A–B). SKMEL-23 cells treated with SB216763 demonstrated a significant increased incidence of apoptotic phenotypes 12 hours post-treatment to 18.40%+/−3.69% of the total population (Fig. 3C) and peaked between 9 and 16 hours of drug treatment but was absent after 24 hours. A similar trend occurred in melanoma lines A375, 624, and 888 with 19.50%+/−5.97%, 25.25%+/−8.50%, and 37.25% +/−8.54% of the total population with apoptotic phenotypes, respectively. In contrast,

apoptotic cells were not observed in 537 or SKMEL-28 cells. SKMEL-23 cells transfected with si*GSK-3*α, si*GSK-3*β, or both also developed apoptotic phenotypes compared to the siScramble control at 18 hours (Fig. 3D–G). While all 3 of the experimental groups were significantly different than siScramble, si*GSK-3*α and both si*GSK-3*α and si*GSK-3*β had similar percentages of apoptotic cells of 11.75%+/−3.47% and 11.51%+/−1.12%, respectively, while inhibition of GSK-3β resulted in a minority population of apoptotic cells (6.31%+/−1.03%, p=0.0070) (Fig. 3H).

A biochemical feature of apoptosis is PARP cleavage. A375, 624, and 888 lines demonstrated truncated PARP protein 12–48 hours post SB216763 treatment (Fig. 3I). PARP cleavage was not detectable in cells that did not display any signs of apoptosis (537, SKMEL-28) and in SKMEL-23 cells. Due to the absence of PARP cleavage in SKMEL-23 cells, we cannot confirm that they undergo apoptosis although they demonstrate typical apoptotic morphology (Fig. 3). These events indicate that inhibition of GSK-3 activity in melanoma cells induces transient apoptotic phenotypes in a subset of melanoma cell lines.

GSK-3 inhibition results in dendritic process extension

SKMEL-23 and 537 cells demonstrated a significant morphological change after GSK-3 inhibition. Both lines showed a SB216763 dose-dependent extension of cell body length and dendritic processes compared to control cells (Fig. 4A–J). After exposure to 20μM SB216763, SKMEL-23 increased cell length to 295.6% +/− 66.3% of control and 537 increased to 242.5% +/− 48.4% of controls. Dendritic process extension observed with SB216763 was replicated when *GSK-3*α, *GSK-3*β, or both were specifically knocked down with siRNA compared to the siScramble control (Fig. 4K–R). SKMEL-23 knockdown of *GSK-3*β and both *GSK-3*α and *GSK-3*β resulted in a significant extension of dendritic processes to 244.89%+/−73.6% and 210.23%+/−64.74% of the length of siScramble cells (Fig. 4S). However, si*GSK-3*α did not cause elongation. Blocking the expression of both isoforms in 537 cells replicated the cellular consequences of SB216763 on cell length with cells elongated to 290.0%+/−133.1% the length of control cells (Fig. 4T). Inhibition of only one *GSK-3* isoform also impacted cell length, although to a lesser extent of blocking both kinases. Inhibition of *GSK-3*α and *GSK-3*β lead to a 226.6%+/−138.3% and 234.4%+/−91.5% increase in cell length in comparison to control, respectively (Fig. 4T). These data indicate that GSK-3 inhibition causes cell elongation.

GSK-3 inhibition leads to a concurrent drop of PAX3 protein

GSK-3 inhibition results in decreased cell growth and an increase in cell and dendritic process length, a feature of melanocyte differentiation. We therefore examined PAX3 levels in melanoma cells since this protein functions in these processes during melanocyte development (17–19). PAX3 levels significantly decreased in all cell lines treated with 20μM SB216763, with decreases in 4/6 cell lines to nearly undetectable levels (Fig. 5A–B). Compared to control, SKMEL-23 (4.97%+/−1.80%), 537 (8.57%+/−4.05%), A375 (11.11% +/−8.50%), and 624 (11.70+/−3.40%) had significant drops in PAX3 levels 72 hours post SB216763. Cell lines 888 and SKMEL-28 had a smaller, yet significant effect on PAX3 levels upon GSK-3 inhibition with 79.90%+/−8.12% (p=0.0251) and 86.47%+/−6.23% (p=0.0320) of control, respectively. We also evaluated the effect of *GSK-3*α and *GSK-3*β knockdown on PAX3 protein levels in SKMEL-23 and 537 cells (Fig. 5C–F). Transfection of SKMEL-23 and 537 cells with si*GSK-3*α or si*GSK-3*β resulted in specific knockdown of the isoform without causing loss of the other isoform. SKMEL-23 cells transfected with si*GSK-3*α, si*GSK-3*β, and both resulted in a loss of over 50% of PAX3 levels compared to siScramble (Fig. 5C–D). Knockdown of either *GSK-3*α or *GSK-3*β in 537 cells reduced the amount of PAX3 protein to 70.2% and 51.8% of the siScramble control, respectively (Fig. 5E–F). The combination of both si*GSK-3*α and si*GSK-3*β further reduced PAX3 levels to

34.9% of control levels. These data suggest that the morphological phenotypes, reduction of cell growth and PAX3 reduction seen with SB216763 was due to the specific inhibition of GSK-3 activity, and that the isoforms have overlapping but non-redundant consequences on PAX3 levels. These data demonstrate that GSK-3 inhibition coincides with a decrease in PAX3 protein levels.

PAX3 possesses three putative GSK-3β triplicate recognition motifs

GSK-3 phosphorylates the consensus sequence T/S-X_3-S/T with prerequisite phosphorylation on the C-terminal S/T by other kinases as for substrates β-catenin and glycogen synthase (1, 33). Alternatively, negatively charged amino acids surrounding the target site bypass the requirement of another kinase (1). β-catenin possesses a series of consecutive consensus motifs, which are phosphorylated by GSK-3β in a sequential manner using pre-phosphorylated Ser45 as a priming point, a pattern also seen in glycogen synthase (34). The PAX3 amino acid sequence contains three independent putative GSK-3β triplicate recognition motifs, which are highly conserved between mouse and human (Fig. 6A). Of interest, Ser209 and Ser213 are surrounded by negatively charged amino acids, which may provide a phosphorylation mimic sometimes required for GSK-3β activity. The identification of this consensus motif is highly suggestive that PAX3 might be a target of GSK-3β.

GSK-3β interacts with PAX3 *in-vitro*

The presence of three different GSK-3β recognition motif series within the PAX3 protein lead us to investigate if these proteins directly interact. In immunoprecipitation experiments, neither PAX3 nor HA-tagged GSK-3β bound to the beads alone (Fig. 6B). In the presence of HA antibody, HA-tagged GSK-3β alone or in combination with PAX3 were immunoprecipitated and ran at the expected size as indicated by the input lane (Fig. 6B, lane-6). These data show that GSK-3β and PAX3 interact *in-vitro*.

GSK-3β phosphorylates PAX3

Since PAX3 directly binds to GSK-3β and contains potential GSK-3β phosphorylation sites, we tested if PAX3 is a GSK-3β substrate. Mouse and human PAX3 share 98% homology and possess a paired domain (PD), octapeptide (O) and homeodomain (HD) (Fig. 6C) (35). Of the three possible GSK-3β consensus motifs within PAX3, site1 was the primary focus since it has been previously determined that PAX3 is phosphorylated at Ser205 (27, 28). Three different GST-PAX3 fusion proteins were tested for phosphorylation: pGex2T-PAX3PDHD-WT, which includes the full PAX3 except for the first 33 amino acids and amino acids 298–484 of the C-terminal tail, pGex2T-PAX3PDHD-ΔSERAS, which is identical to pGex2T-PAX3PDHD-WT but with a deletion of a peptide segment containing putative GSK-3β recognition site1, and pGex2T-PAX3PD, that only includes the N-terminal of PAX3 and does not include site1 (Fig. 6C). pGex2T-PAX3PDHD-WT was the only construct phosphorylated in the presence (Fig. 6D, lane-4) but not in the absence of GSK-3β (lane-3). Absence of PAX3 (Fig. 6D, lane-1,2), or protein without the site1 epitope (lanes-5–8) or without GSK-3β (lanes-1,3,5,7) failed to produce a phosphorylated band of the expected size. All samples with GSK-3β also produced a higher molecular weight band, most likely due to auto-phosphorylation and carry-over of GSK-3β (36). These findings demonstrate that GSK-3β phosphorylates PAX3 within the first series of GSK-3β recognition motifs.

To complement the *in-vitro* phosphorylation studies, we tested if endogenous GSK-3 within melanoma lysates was capable of phosphorylating PAX3 and found the addition of SB216763 reduced PAX3 phosphorylation in most, but not in all cell lines tested (Supplementary Fig. S3). These findings correlate with the cellular response of PAX3 loss

due to GSK inhibition (Fig. 5), and that melanoma cell lysates contain components that can mimic the function of exogenous GSK-3 (Fig. 6).

GSK-3β-phosphorylated pGex2T-PAX3PDHD-WT protein was analyzed by mass spectroscopy (MS) to identify modified amino acids. The MS/MS signature not only determined that peptides derived from the region shown in Figure 6 are phosphorylated, but are so on multiple residues: Ser205 (Fig. 6E) and either Ser197 or Ser201 (Fig. 6F). Strict criteria were used to manually evaluate and identify sites of phosphorylation (see Supplementary methods), which provide support for phosphorylation at Ser205 and Ser197 or Ser201. Phosphorylation at site Ser197 or Ser201 could not be determined specifically due to poor b-ion spectra (Fig. 6F) and each moiety received nearly the same mascot peptide score, 22 for Ser197 and 19 for Ser201, thus both sites have been included as the possible single phosphorylation event (Supplementary Fig. S4). Evidence for phosphorylation of Ser193 was not detected, although this may be due to trypsin cleavage proximal to this epitope. Based on our protein kinase assays, MS data and the GSK-3 consensus sequence within the PAX protein, we conclude that GSK-3β binds to PAX3 and phosphorylates serine residues (Ser205 and either Ser197 or Ser201) without the requirement of another kinase to prime the first C-terminal site. This data suggests that GSK-3β does not require a priming phosphorylation to target PAX3 *in-vitro*, since there were no other components in the kinase assay mixture that could supply such a priming event and that the negatively charged amino acids surrounding Ser209 in PAX3 are sufficient to mimic a phospho-primed substrate.

PAX3 knockdown mimics cell phenotypes of GSK-3 inhibition

SKMEL-23 and 537 cells were transfected with si*PAX3* or siScramble to assess whether the phenotypes exhibited with GSK-3 inhibition was a result of the reduction in PAX3 levels (Fig. 7A–D). At 72 hours cells transfected with si*PAX3* had significantly fewer cells than those transfected with siScramble; 41.89%+/−8.10% (SKMEL-23) and 52.83%+/−11.46% (537) (Fig. 7E). PAX3 knockdown also had the same effect as GSK-3 inhibition for cell length where SKMEL-23 (202.78%+/−78%) and 537 cells (237.96%+/−85.5%) were significantly longer than siScramble transfected controls (Fig. 7F). Western blots verified that the si*PAX3* effectively knocked down PAX3 levels in the transfected cells (Fig. 7G–H, Supplementary Fig. S1D).

Maintenance of PAX3 levels protects cells from cellular consequences of GSK-3 inhibition

To determine if the outcome of GSK-3 inhibition is dependent on PAX3 loss in SKMEL-23 and 537 melanoma cells, exogenous PAX3 was expressed within these cells. Both SKMEL-23 and 537 cells were transfected with either empty expression vector pcDNA3 or pcDNA3-PAX3-HA and treated with DMSO or SB216763 (Figure 7I–P). Western blots confirm the expression of PAX3-HA in cells transfected with pcDNA3-PAX3-HA but not in cells with empty pcDNA3 (Supplementary Fig. S5). Cells transfected with pcDNA3 responded to treatment in the same way as untransfected cells (Fig. 2,4,7). Cells transfected with pcDNA3-PAX3-HA, however, were protected from the effects of SB216763 and GSK-3 inhibition. After 72 hours of SB216763 treatment, cell numbers for PAX3-HA expressing cells were 139.51%+/−16.02% (SKMEL-23) or 125.82%+/− 8.15% (537) in comparison to untreated pcDNA3 cells (set at 100%), in comparison to 32.96%+/−6.99% (SKMEL-23) or 38.08%+/−3.76% (537) of pcDNA3 transfected and SB216763-treated cells (Fig. 7Q–R). In parallel, while pcDNA3 cells became elongated after SB216763 treatment much like prior experiments (Fig.4, 7S–T), PAX3-HA expressing cells demonstrated no overt morphological changes. In contrast, both cell types display a trend towards a shorter, more rounded cell shape. These data shows that PAX3 over-expression rescues the phenotypes of GSK-3 inhibition. All of these data collectively support a model in which

GSK-3 inhibition in melanoma cells results in cell growth reduction, cell elongation, and apoptosis with PAX3 modulating cell growth and cell length (Fig. 7U).

Discussion

GSK-3 inhibition influences human melanoma cell growth, apoptosis and morphology

In this report, GSK-3α and GSK-3β actively promoted melanoma cell growth, despite phosphorylation at Ser21 or Ser9 in the majority of cell lines. While phosphorylation at these sites are indicative of GSK-3 inactivation for some targets, this phosphorylation state does not completely inactivate GSK-3 within melanoma since small molecule inhibition or siRNA-mediated knockdown of GSK-3 lead to alteration of cell growth, survival, and cell morphology. GSK-3 inhibition is associated with decreased proliferation and increased apoptosis in several cancers including mouse melanoma (15). Consistent with these previous findings, we found that 5/6 human melanoma cell lines exhibited slower proliferative rates as a result of GSK-3 inhibition (Fig. 2, Supplementary Fig. S2). While apoptosis was observed upon GSK-3 inhibition, any apoptotic cell death measured in these studies were transient and did not exceed 35% of the total population, with the exception of 888 cells. Out of the four cell lines that presented with apoptotic phenotypes, three displayed measurable PARP cleavage. SKMEL-23 cells demonstrated apoptotic morphology but no evidence of PARP cleavage was measured. These changes in cellular proliferation and survival might be due to genes associated with GSK-3 activity including NF-κB, Bcl-2 and XIAP (37–39).

Both SKMEL-23 and 537 human melanoma cell lines also displayed altered morphology upon GSK-3 inhibition, including an increase in overall cell length (Fig. 4) in similarity to responses by normal human melanocytes and mouse melanoma cells (15). This elongation of dendritic processes suggests that GSK-3 plays a role as a control point in terminal differentiation (40). Interestingly, inhibition of either GSK-3 isoform in 537 cells allowed for a reduction in cell growth and an increase in dendritic process length but a block of both isoforms resulted in a more severe phenotype, suggesting that GSK-3α and GSK-3β partially compensated for the loss of the other in this melanoma cell line. In SKMEL-23 cells, however, this phenotype was more dependent on GSK-3β.

GSK-3β phosphorylates PAX3 and is correlated with PAX3 levels in melanoma

PAX3 plays many critical roles in melanocyte precursors during development including proliferation, resistance to apoptosis and regulation of terminal differentiation, all characteristics altered by GSK-3 inhibition (18, 20). Mouse embryos that lack PAX3 have increased levels of apoptotic cell bodies, linking PAX3 with cellular survival (41). Further, reduction of PAX3 expression in melanoma cell lines results in slowed growth and induction of apoptosis (20, 24). Attenuation of GSK-3 activity resulted in PAX3 protein loss in 4/6 melanoma cell lines (Fig. 5). In addition, specific knockdown of each *GSK-3* isoform decreased PAX3 levels in SKMEL-23 and 537 cells. Double knockdowns resulted in even lower PAX3 for 537 cells, indicating that the GSK-3 isoforms incompletely compensated for each other in regards to PAX3 levels in this cell line. Cell growth reduction and dendritic process extension correlated with the loss of PAX3 through either GSK-3 inhibition or siPAX3. Further, exogenous PAX3 expression rescued these phenotypes, suggesting that PAX3 levels is one mechanism through which GSK-3 regulates proliferative rates in melanoma cell lines. It is reasonable to predict that PAX3 plays a role in the apoptosis caused by the inhibition of GSK-3, due to prior studies finding PAX3-dependent apoptosis in melanoma (20, 24). However, in our studies, we do not see evidence of apoptosis after inhibition of PAX3 expression. In contrast, the most dramatic induction of apoptosis due to GSK-3 inhibition seen was in the 888 cell line, where no significant reduction in PAX3 was

measured. The difference between our finding and the prior reports is most likely due to differences in cell lines, since melanoma cells are notoriously heterogeneous in their responses to treatments and in gene expression. While our data support that PAX3 is involved in GSK-3-mediated growth, a role for PAX3 in GSK-3-dependent cell survival was not established (Fig. 7U).

Maintenance of PAX3 levels was dependent on GSK-3 activity in melanoma cell lines and GSK-3β phosphorylated PAX3 at multiple residues (Fig. 5–6). GSK-3β phosphorylation can lead to protein degradation, such as with β-catenin (42). However, there are numerous examples of GSK-3β phosphorylation leading to protein stabilization and activation. In the colon, GSK-3β can alter phosphorylation targets from β-catenin to Hath1, thereby toggling cellular activity between proliferation and differentiation (43). A similar trend is seen during Wnt signaling where activation causes GSK-3β to phosphorylate LRP6 instead of β-catenin, thereby activating this receptor, allowing for continuation of the Wnt signal (44). GSK-3β also modulates Mitf transcription factor activity via phosphorylation of Ser298 (45). Here, the data support that one function for GSK-3 in melanoma cells is to maintain PAX3, thereby promoting tumor progression and survival.

Other post-transcriptional modifications of PAX3 have been discovered that effect protein function and stability. These studies focused on the role of PAX3 in muscle rather than melanocytes or melanoma, and often focus on the PAX3/FOXO1 translocation product in alveolar rhabdomyosarcoma (46). PAX3/FOXO1 is phosphorylated at multiple sites in the PAX3 portion of the protein by an unidentified kinase, modulating its ability to act upon downstream target genes (25). During myocyte development, PAX3 levels must decrease in order for terminal differentiation to occur as a result of post-translational alterations in protein stability (26, 47). The ubiquitination and proteasomal degradation pathway also regulates PAX3 stability by targeting monoubiquitinated PAX3 for degradation within myogenic precursor cells, thus allowing differentiation at the proper time during development (47). PAX3 levels are increased in order to drive quiescent muscle satellite cells further toward a myocytic fate. PAX3 is phosphorylated at multiple sites including Ser205 in mouse primary myoblasts and this phosphorylation is lost upon the progression of the differentiation program (27). A recent report finds Ser201, Ser205 and Ser209 are phosphorylated in PAX3, due to CK2 (formerly casein kinase II) at Ser205 and GSK-3β at Ser 201 with phosphorylation status affecting myogenic differentiation progression (29). The ubiquitously expressed CK2 often provides the priming phosphorylation for GSK-3, however, we found that GSK-3β alone was sufficient to phosphorylate PAX3 at both Ser205 and Ser197/Ser201 *in-vitro* (33, 48). A similar system of PAX3 regulation may occur in melanoblast development into melanocytes and in melanoma. While our studies find that PAX3 is phosphorylated by GSK-3 in melanoma cells, the effect of this phosphorylation on PAX3 protein function still needs to be determined.

Over the course of this study, we found that GSK-3 inhibition in melanoma cells dramatically reduced cell growth, increased apoptosis and altered morphology to mimic differentiated melanocytes. We found that the cell growth reduction and altered morphology may have been due, in part, to reduction of PAX3. We also established that GSK-3α and GSK-3β are phosphorylated at Ser21 and Ser9 in melanoma cells, but are active kinases supporting cellular growth. In addition, both isoforms of GSK-3 can compensate for each other in regard to cell growth and PAX3 levels. Now that a link has been established between GSK-3 activity and PAX3 levels in melanoma cells, future experimentation will assess if the interplay between these two proteins is directly responsible for providing attributes necessary for melanoma growth and survival. Elucidation of the pathway allowing for the proliferation, survival and differentiation resistance in melanoma will be key to

providing improved targeted therapy for this disease that is increasing in incidence worldwide every year.

Supplementary Material

Refer to Web version on PubMed Central for supplementary material.

Acknowledgments

The authors are grateful to Jonathan A. Epstein, Kurt Engleka (University of Pennsylvania), Igor B. Dawid (National Institutes of Health), Christopher R. Shea, Keyoumars Soltani, and Erica L. Littlejohn (University of Chicago) for reagents and/or scientific input. We would like to acknowledge Ken Johnson for LC-MS/MS data acquisition on the Orbitrap-LTQ at the Mayo Proteomics Research Center, Mayo Clinic and Foundation.

Financial support: The Schweppe Foundation, University of Chicago Cancer Center Pilot program (P30-CA014599), American Skin Association, American Cancer Society (RSG-CSM-121505), Friends of Dermatology-University of Chicago, Outrun the Sun, Inc., and National Institutes of Health (R01CA130202).

References

1. Doble BW, Woodgett JR. GSK-3: tricks of the trade for a multi-tasking kinase. J Cell Sci. 2003; 116:1175–1186. [PubMed: 12615961]
2. Woodgett JR. Molecular cloning and expression of glycogen synthase kinase-3/factor A. EMBO J. 1990; 9:2431–2438. [PubMed: 2164470]
3. Yao HB, Shaw PC, Wong CC, Wan DC. Expression of glycogen synthase kinase-3 isoforms in mouse tissues and their transcription in the brain. J Chem Neuroanat. 2002; 23:291–297. [PubMed: 12048112]
4. Lau KF, Miller CC, Anderton BH, Shaw PC. Expression analysis of glycogen synthase kinase-3 in human tissues. J Pept Res. 1999; 54:85–91. [PubMed: 10448973]
5. Sutherland C, Leighton IA, Cohen P. Inactivation of glycogen synthase kinase-3 beta by phosphorylation: new kinase connections in insulin and growth-factor signalling. Biochem J. 1993; 296(Pt 1):15–19. [PubMed: 8250835]
6. Sutherland C, Cohen P. The alpha-isoform of glycogen synthase kinase-3 from rabbit skeletal muscle is inactivated by p70 S6 kinase or MAP kinase-activated protein kinase-1 in vitro. FEBS Lett. 1994; 338:37–42. [PubMed: 8307153]
7. Ding VW, Chen RH, McCormick F. Differential regulation of glycogen synthase kinase 3beta by insulin and Wnt signaling. J Biol Chem. 2000; 275:32475–32481. [PubMed: 10913153]
8. Doble BW, Patel S, Wood GA, Kockeritz LK, Woodgett JR. Functional redundancy of GSK-3alpha and GSK-3beta in Wnt/beta-catenin signaling shown by using an allelic series of embryonic stem cell lines. Dev Cell. 2007; 12:957–971. [PubMed: 17543867]
9. Hoeflich KP, Luo J, Rubie EA, Tsao MS, Jin O, Woodgett JR. Requirement for glycogen synthase kinase-3beta in cell survival and NF-kappaB activation. Nature. 2000; 406:86–90. [PubMed: 10894547]
10. Liu KJ, Arron JR, Stankunas K, Crabtree GR, Longaker MT. Chemical rescue of cleft palate and midline defects in conditional GSK-3beta mice. Nature. 2007; 446:79–82. [PubMed: 17293880]
11. Kerkela R, Kockeritz L, Macaulay K, Zho J, Doble BW, Beahm C, et al. Deletion of GSK-3beta in mice leads to hypertrophic cardiomyopathy secondary to cardiomyoblast hyperproliferation. J Clin Invest. 2008; 118:3609–3618. [PubMed: 18830417]
12. MacAulay K, Doble BW, Patel S, Hansotia T, Sinclair EM, Drucker DJ, et al. Glycogen synthase kinase 3alpha-specific regulation of murine hepatic glycogen metabolism. Cell Metab. 2007; 6:329–337. [PubMed: 17908561]
13. Chien AJ, Moore EC, Lonsdorf AS, Kulikauskas RM, Rothberg BG, Berger AJ, et al. Activated Wnt/beta-catenin signaling in melanoma is associated with decreased proliferation in patient tumors and a murine melanoma model. Proc Natl Acad Sci U S A. 2009; 106:1193–1198. [PubMed: 19144919]

14. Panka DJ, Cho DC, Atkins MB, Mier JW. GSK-3beta inhibition enhances sorafenib-induced apoptosis in melanoma cell lines. J Biol Chem. 2008; 283:726–732. [PubMed: 17991738]
15. Bellei B, Flori E, Izzo E, Maresca V, Picardo M. GSK3beta inhibition promotes melanogenesis in mouse B16 melanoma cells and normal human melanocytes. Cell Signal. 2008; 20:1750–1761. [PubMed: 18602000]
16. Jin EJ, Erickson CA, Takada S, Burrus LW. Wnt and BMP signaling govern lineage segregation of melanocytes in the avian embryo. Dev Biol. 2001; 233:22–37. [PubMed: 11319855]
17. Watanabe A, Takeda K, Ploplis B, Tachibana M. Epistatic relationship between Waardenburg syndrome genes MITF and PAX3. Nat Genet. 1998; 18:283–286. [PubMed: 9500554]
18. Lang D, Lu MM, Huang L, Engleka KA, Zhang M, Chu EY, et al. Pax3 functions at a nodal point in melanocyte stem cell differentiation. Nature. 2005; 433:884–887. [PubMed: 15729346]
19. Hornyak T, Hayes D, Chiu L-Y, Ziff E. Transcription factors in melanocyte development: distinct roles for Pax-3 and Mitf. Mechanisms of Development. 2001; 101:47–59. [PubMed: 11231058]
20. Scholl FA, Kamarashev J, Murmann OV, Geertsen R, Dummer R, Schafer BW. PAX3 is expressed in human melanomas and contributes to tumor cell survival. Cancer Res. 2001; 61:823–826. [PubMed: 11221862]
21. Plummer RS, Shea CR, Nelson M, Powell SK, Freeman DM, Dan CP, et al. PAX3 expression in primary melanomas and nevi. Mod Pathol. 2008; 21:525–530. [PubMed: 18327212]
22. Mascarenhas JB, Littlejohn EL, Wolsky RJ, Young KP, Nelson M, Salgia R, et al. PAX3 and SOX10 activate MET receptor expression in melanoma. Pigment Cell Melanoma Res. 2010; 23:225–237. [PubMed: 20067553]
23. Natali PG, Nicotra MR, Di Renzo MF, Di Renzo MF, Prat M, Bigotti A, et al. Expression of the c-Met/HGF receptor in human melanocytic neoplasms: demonstration of the relationship to malignant melanoma tumour progression. Br J Cancer. 1993; 68:746–750. [PubMed: 8104462]
24. He SJ, Stevens G, Braithwaite AW, Eccles MR. Transfection of melanoma cells with antisense PAX3 oligonucleotides additively complements cisplatin-induced cytotoxicity. Mol Cancer Ther. 2005; 4:996–1003. [PubMed: 15956257]
25. Amstutz R, Wachtel M, Troxler H, Kleinert P, Ebauer M, Haneke T, et al. Phosphorylation regulates transcriptional activity of PAX3/FKHR and reveals novel therapeutic possibilities. Cancer Res. 2008; 68:3767–3776. [PubMed: 18483260]
26. Miller PJ, Hollenbach AD. The oncogenic fusion protein Pax3-FKHR has a greater post-translational stability relative to Pax3 during early myogenesis. Biochim Biophys Acta. 2007; 1770:1450–1458. [PubMed: 17698292]
27. Miller PJ, Dietz KN, Hollenbach AD. Identification of serine 205 as a site of phosphorylation on Pax3 in proliferating but not differentiating primary myoblasts. Protein Sci. 2008; 17:1979–1986. [PubMed: 18708529]
28. Dietz KN, Miller PJ, Hollenbach AD. Phosphorylation of serine 205 by the protein kinase CK2 persists on Pax3-FOXO1, but not Pax3, throughout early myogenic differentiation. Biochemistry. 2009; 48:11786–11795. [PubMed: 19904978]
29. Dietz KN, Miller PJ, Iyengar AS, Loupe JM, Hollenbach AD. Identification of serines 201 and 209 as sites of Pax3 phosphorylation and the altered phosphorylation status of Pax3-FOXO1 during early myogenic differentiation. Int J Biochem Cell Biol. 2011; 43:936–945. [PubMed: 21440083]
30. He X, Saint-Jeannet JP, Woodgett JR, Varmus HE, Dawid IB. Glycogen synthase kinase-3 and dorsoventral patterning in Xenopus embryos. Nature. 1995; 374:617–622. [PubMed: 7715701]
31. Lang D, Epstein JA. Sox10 and Pax3 physically interact to mediate activation of a conserved c-RET enhancer. Hum Mol Genet. 2003; 12:937–945. [PubMed: 12668617]
32. Coghlan MP, Culbert AA, Cross DA, Corcoran SL, Yates JW, Pearce NJ, et al. Selective small molecule inhibitors of glycogen synthase kinase-3 modulate glycogen metabolism and gene transcription. Chem Biol. 2000; 7:793–803. [PubMed: 11033082]
33. Fiol CJ, Wang A, Roeske RW, Roach PJ. Ordered multisite protein phosphorylation. Analysis of glycogen synthase kinase 3 action using model peptide substrates. J Biol Chem. 1990; 265:6061–6065. [PubMed: 2156841]

34. Hagen T, Di Daniel E, Culbert AA, Reith AD. Expression and characterization of GSK-3 mutants and their effect on beta-catenin phosphorylation in intact cells. J Biol Chem. 2002; 277:23330–23335. [PubMed: 11967263]
35. Kubic JD, Young KP, Plummer RS, Ludvik AE, Lang D. Pigmentation PAX-ways: the role of Pax3 in melanogenesis, melanocyte stem cell maintenance, and disease. Pigment Cell Melanoma Res. 2008; 21:627–645. [PubMed: 18983540]
36. Turenne GA, Price BD. Glycogen synthase kinase3 beta phosphorylates serine 33 of p53 and activates p53's transcriptional activity. BMC Cell Biol. 2001; 2:12. [PubMed: 11483158]
37. Ougolkov AV, Fernandez-Zapico ME, Bilim VN, Smyrk TC, Chari ST, Billadeau DD. Aberrant nuclear accumulation of glycogen synthase kinase-3beta in human pancreatic cancer: association with kinase activity and tumor dedifferentiation. Clin Cancer Res. 2006; 12:5074–5081. [PubMed: 16951223]
38. Ougolkov AV, Fernandez-Zapico ME, Savoy DN, Urrutia RA, Billadeau DD. Glycogen synthase kinase-3beta participates in nuclear factor kappaB-mediated gene transcription and cell survival in pancreatic cancer cells. Cancer Res. 2005; 65:2076–2081. [PubMed: 15781615]
39. Bilim V, Ougolkov A, Yuuki K, Naito D, Kawazoe H, Muto A, et al. Glycogen synthase kinase-3: a new therapeutic target in renal cell carcinoma. Br J Cancer. 2009; 101:2005–2014. [PubMed: 19920820]
40. Romero-Graillet C, Aberdam E, Clement M, Ortonne JP, Ballotti R. Nitric oxide produced by ultraviolet-irradiated keratinocytes stimulates melanogenesis. J Clin Invest. 1997; 99:635–642. [PubMed: 9045865]
41. Phelan SA, Ito M, Loeken MR. Neural tube defects in embryos of diabetic mice: role of the Pax-3 gene and apoptosis. Diabetes. 1997; 46:1189–1197. [PubMed: 9200655]
42. Aberle H, Bauer A, Stappert J, Kispert A, Kemler R. beta-catenin is a target for the ubiquitin-proteasome pathway. EMBO J. 1997; 16:3797–3804. [PubMed: 9233789]
43. Tsuchiya K, Nakamura T, Okamoto R, Kanai T, Watanabe M. Reciprocal targeting of Hath1 and beta-catenin by Wnt glycogen synthase kinase 3beta in human colon cancer. Gastroenterology. 2007; 132:208–220. [PubMed: 17241872]
44. Zeng X, Tamai K, Doble B, Li S, Huang H, Habas R, et al. A dual-kinase mechanism for Wnt co-receptor phosphorylation and activation. Nature. 2005; 438:873–877. [PubMed: 16341017]
45. Takeda K, Takemoto C, Kobayashi I, Watanabe A, Nobukuni Y, Fisher DE, et al. Ser298 of MITF, a mutation site in Waardenburg syndrome type 2, is a phosphorylation site with functional significance. Hum Mol Genet. 2000; 9:125–132. [PubMed: 10587587]
46. Barr FG, Galili N, Holick J, Biegel JA, Rovera G, Emanuel BS. Rearrangement of the PAX3 paired box gene in the paediatric solid tumour alveolar rhabdomyosarcoma. Nat Genet. 1993; 3:113–117. [PubMed: 8098985]
47. Boutet SC, Disatnik MH, Chan LS, Iori K, Rando TA. Regulation of Pax3 by proteasomal degradation of monoubiquitinated protein in skeletal muscle progenitors. Cell. 2007; 130:349–362. [PubMed: 17662948]
48. Olsten ME, Litchfield DW. Order or chaos? An evaluation of the regulation of protein kinase CK2. Biochem Cell Biol. 2004; 82:681–693. [PubMed: 15674436]

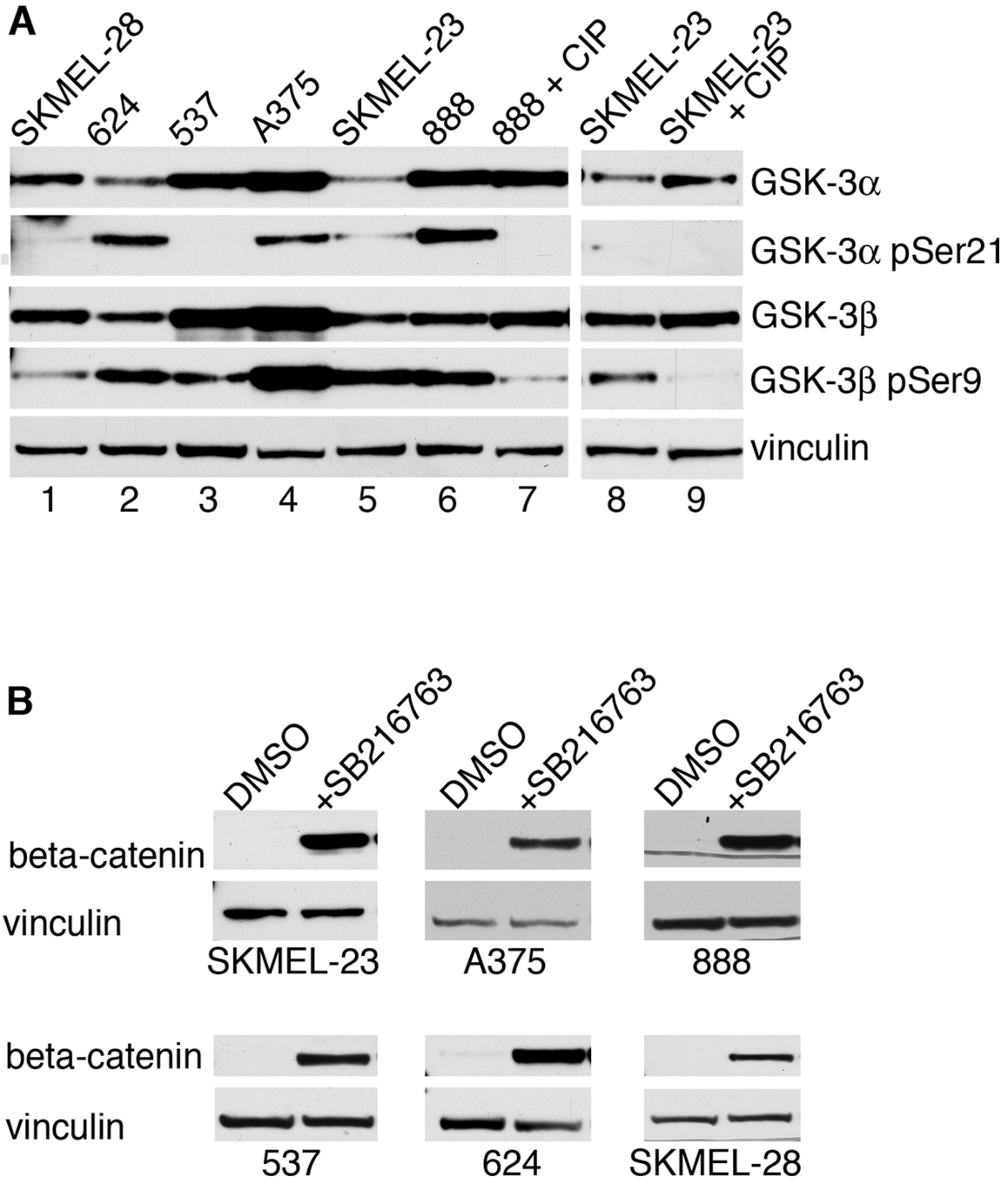

Figure 1.

GSK-3 status in melanoma cell lines. A, melanoma cell lines express both GSK-3α and GSK-3β at varying levels of phosphorylation. Western blots of melanoma lysates were probed with antibodies recognizing total and phosphorylated GSK-3α and GSK-3β. Lysates from 888 and SKMEL-23 cells were treated with calf intestinal phosphatase (CIP) as controls for phospho-Ser9 and phospho-Ser21. B, GSK-3 inhibition raises β-catenin levels. Melanoma cell lines treated with DMSO or SB216763, for 24 hours were probed with β-catenin antibody or vinculin antibody as a loading control.

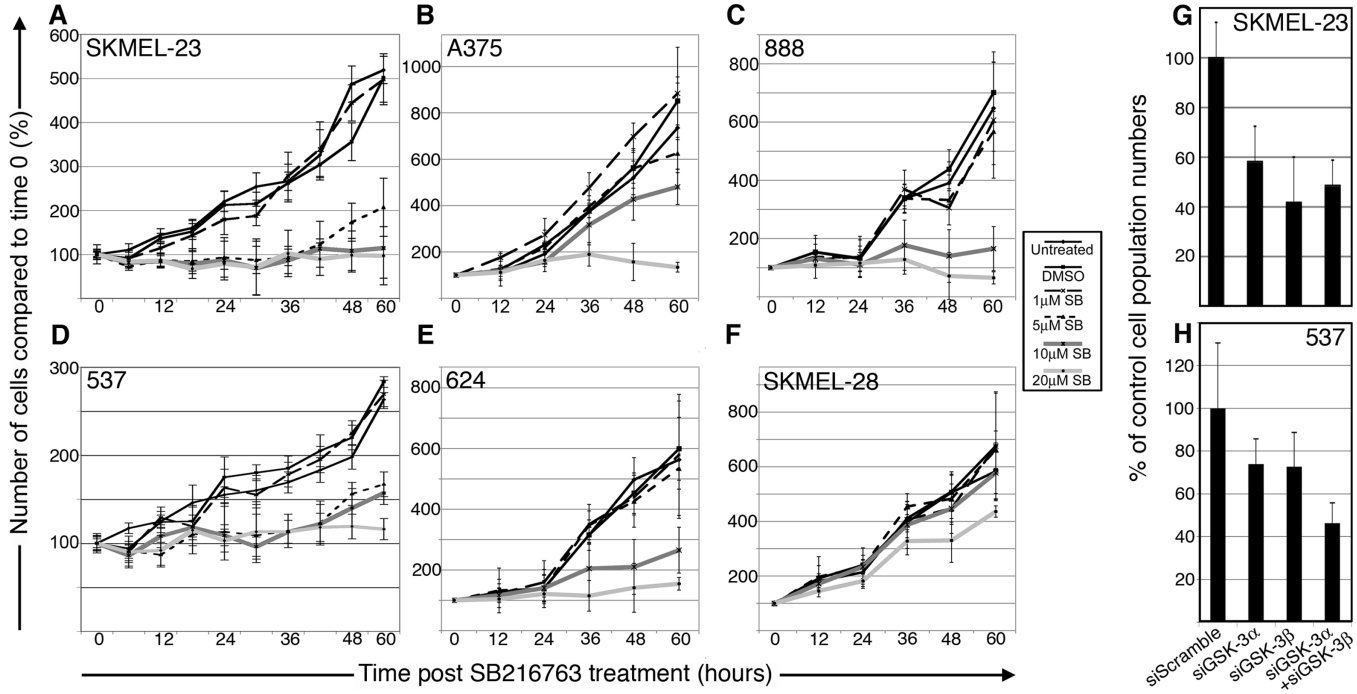

Figure 2.

GSK-3 inhibition results in a dose-dependent cell number reduction. A–F, melanoma cell numbers over 60 hours of treatment. Cells were left untreated, carrier-treated (DMSO) or with increasing concentrations of SB216763. Cells were counted at commencement of treatment and at 12-hour intervals up to 60 hours. The number of cells at time 0 for each group was set as 100% and the cell counts for all treatment groups are expressed as a percentage of that start value. Values are means +/− s.d. G–H, *GSK-3*α and *GSK-3*β knockdown reduces cell numbers in SKMEL-23 (G) and 537 (H). Cells transfected with si*GSK-3*α, si*GSK-3*β, and both were counted 72 hours post-transfection and compared to siScramble (set at 100%). Values are means +/− s.d. (n=600).

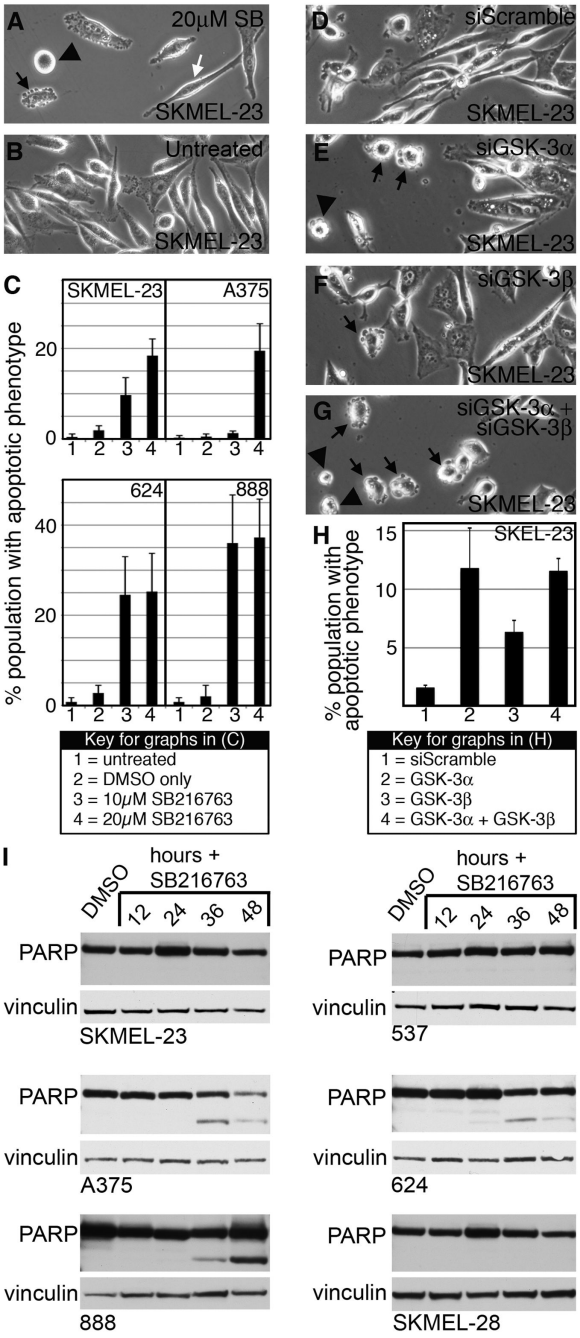

Figure 3.

GSK-3 inhibition induces apoptosis in melanoma cells. A–B, overall morphology of SKMEL-23 cells with (A) or without (B) SB216763 treatment at 9 hours. Cells displayed apoptotic phenotypes including blebbing (black arrow), rounding and adhesion loss (black arrowhead), as well as cells that maintain the parental phenotype (white arrow). C, quantification of apoptotic characteristics in melanoma cell lines upon GSK-3 inhibition. In six random fields, total cells and apoptotic cells were counted and graphed as a percentage of total population. Values are mean +/− s.d. (n=600 cells). D–G, SKMEL-23 cells transfected with siScramble (D), si*GSK-3*α (E), si*GSK-3*β (F), and both isoforms (G) were examined for apoptotic phenotypes 18 hours post-transfection. H, quantification of apoptotic

phenotypes in D–G. Values are means +/− s.d. (n=900 cells) I, Western blots of melanoma cell lines treated with SB216763 for 12–48 hours compared to DMSO controls. Blots were probed with PARP antibody or vinculin antibody as a loading control.

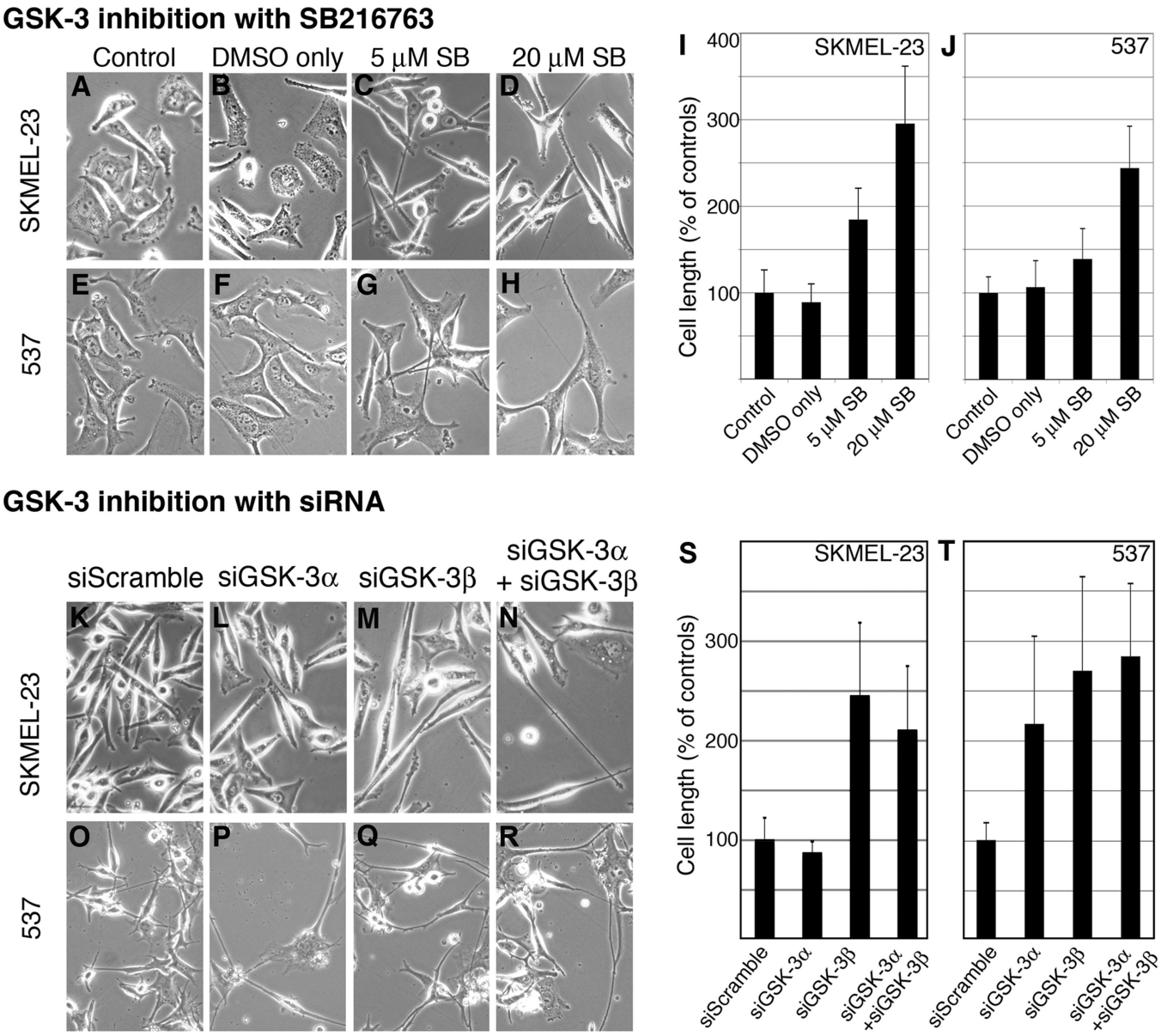

Figure 4.

GSK-3 inhibition with SB216763 or siRNA elongates dendritic processes. A–H, morphology of controls and SB216763-treated SKMEL-23 (A–D) and 537 (E–H) cells. Cells were either untreated (A, E), treated with DMSO (B, F) or with 5μM (C, G) or 20μM (D, H) SB216763 for 60 hours. I–J, quantification of SKMEL-23 and 537 cell length. For each group, 50 cells were measured length-wise and the averaged length of the control cells (A, E) was set at 100%. The presented graph is a compilation of two experiments. Values are means +/− s.d. (n=50). K-R, overall morphology of SKMEL-23 (K–N) and 537 (O–R) cells transfected with siScramble (K, O), si*GSK-3*α (L, P), si*GSK-3*β (M, Q), or both (N, R). Transfected cells exhibited dendritic process extension for both GSK-3 isoforms compared to the control at 72 hours. S–T, quantification of cell length of SKMEL-23 (S) and 537 (T). For each treatment, 10 cells were measured from 6 groups. The experimental groups were expressed as a percentage of the control group (average set at 100%). Values are means +/− s.d. (n=60 cells).

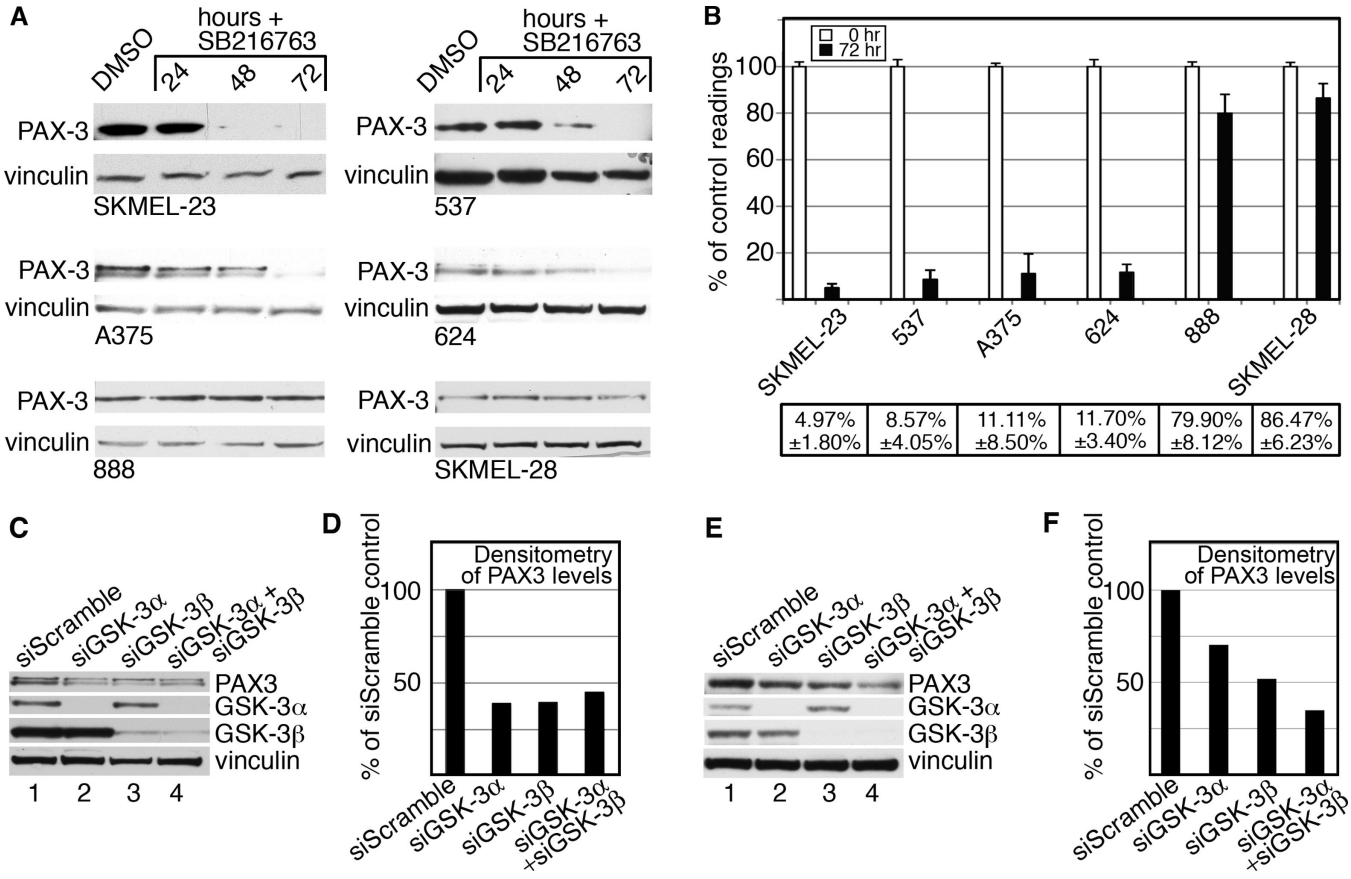

Figure 5.

GSK-3 inhibition is correlated with a decrease in PAX3 levels. A, western blots of melanoma cell lines treated with SB216763. Cells were treated with DMSO or 20μM SB216763 for 24, 48 and 72 hours. Blots were probed with PAX3 antibody or vinculin antibody as a loading control. B, densitometry readings of western blots. The percentage shown represents the levels of PAX3 at 72 hours of treatment (black bars) compared to control (white bars). Values are means +/− s.d. (n=3 independent Western analyses). C–F, specific knockdown of *GSK-3*α and *GSK-3*β reduces PAX3 levels. PAX3 and GSK-3 protein levels were measured in whole-cell lysates from SKMEL-23 (C) and 537 (E) cells transfected with si*GSK-3*α, si*GSK-3*β, both, or siScramble. Blots were probed with PAX3, GSK-3α, GSK-3β, or vinculin antibodies. Densitometry of the PAX3 protein band intensity form SKMEL-23 (D) and 537 (F) are graphed with the siScramble control levels set at 100%.

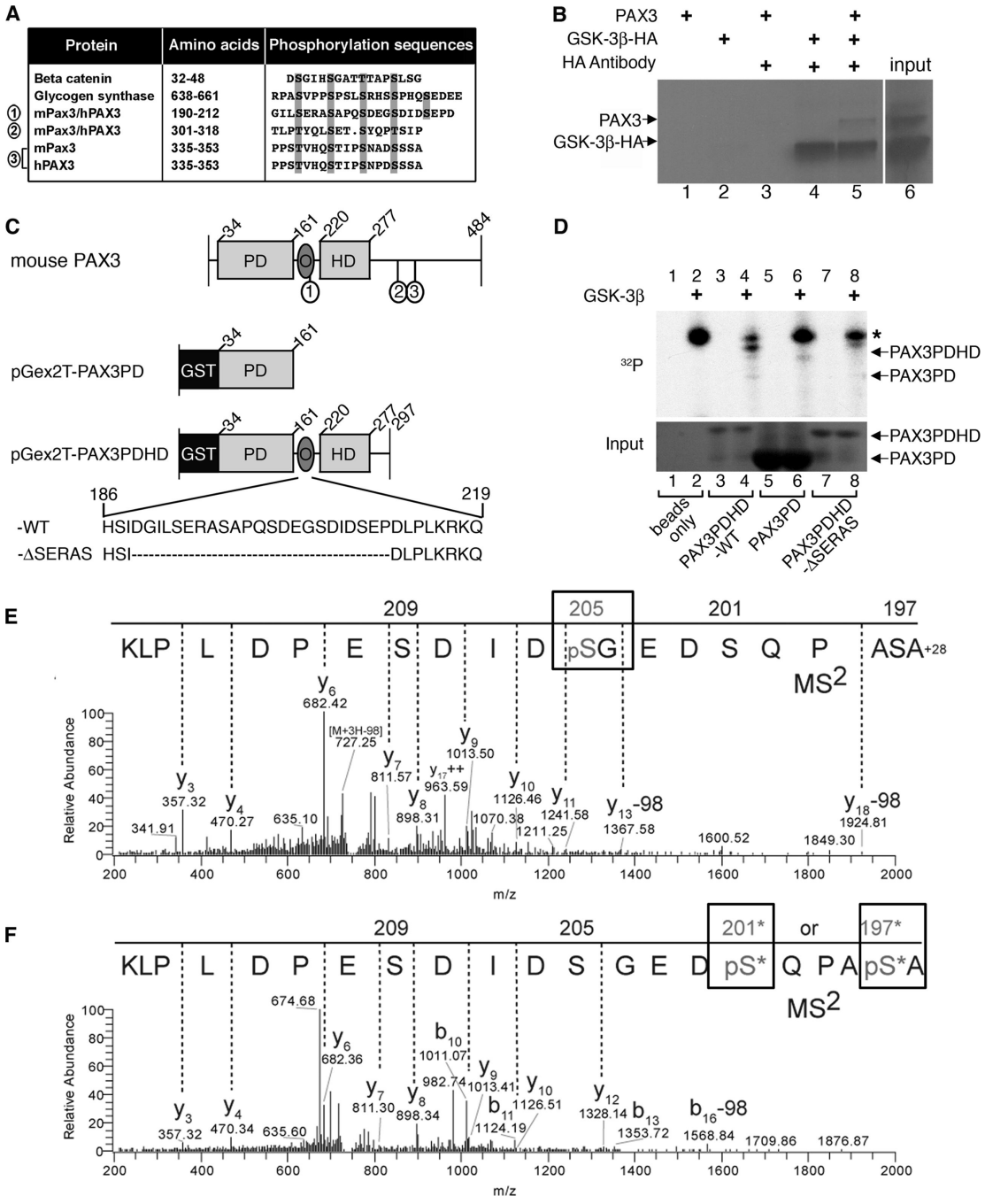

Figure 6.

GSK-3β interacts with and phosphorylates PAX3. A, PAX3 possesses three conserved putative GSK-3β triplicate recognition motifs (sites 1, 2, 3) which are aligned with known GSK-3β targets β-catenin and glycogen synthase. B, immunoprecipitation of GSK-3β and PAX3. Sepharose-A/G beads were mixed with radiolabeled PAX3 (lane-1), HA-GSK-3β (lane-2), PAX3 with HA antibody (lane-3), HA-GSK-3β with HA antibody (lane-4) and both PAX3 and HA-GSK-3β with HA antibody (lane-5). Input of radiolabeled PAX3 and HA-GSK-3β is shown in lane-6. C, schematic of recombinant GST-tagged murine PAX3 proteins. Full-length wild type mouse PAX3 depicts placement of the three putative GSK-3β recognition motifs (1, 2, 3) corresponding to sites in A. The pGex2T-PAX3PD construct

fuses glutathione S-transferase (GST) to the N-terminal end of the paired domain (PD) and contains amino acids 34–161. pGex2T-PAX3PDHD-WT possesses amino acids 34–297 including the PD, octapeptide (O) and the homeodomain (HD). The amino acid sequence of O and the first GSK-3β recognition motif (S/T-X_3-S/T) is represented (wild-type (WT) sequence shown, amino acids 186–219). The construct pGex2T-PAX3PDHD-ΔSERAS has the entire series of GSK-3β recognition motifs removed (deleted sequence, (−ΔSERAS) sequence shown, with the removal of amino acids 189–211). D, GSK-3β and PAX3 kinase assay. The kinase assay was performed on empty glutathione sepharose-4B beads without (lane-1) or with GSK-3β (lane-2), pGex2T-PAX3PDHD-WT without (lane-3) or with GSK-3β (lane-4), pGex2T-PAX3PD without (lane-5) or with GSK-3β (lane-6) and pGex2T-PAX3PDHD-ΔSERAS minus (lane-7) or plus GSK-3β (lane-8). The top panel displays the kinase assay with an asterisk indicating an auto-phosphorylation band. The bottom panel is a coomassie-stained gel visualizing the input bound to the beads. E–F, tandem mass spectrometry determines Ser205 and Ser197/Ser201 of PAX3 are phosphorylated by GSK-3β *in-vitro*. Precursor ion masses were measured in the Orbitrap analyzer and MS^2 spectra were acquired in the LTQ mass spectrometer. E, MS^2 spectra of pSer205 (n-formyl) ASAPQSDEGpSDIDSEPDLPLK (MS mass deviation, 12 ppm). F, MS^2 spectra of peptide AS*APQS*DEGSDIDSEPDLPLK phosphorylated at either Ser197 or Ser201 (MS mass deviation, 23 ppm). The presence of ion Y12 at mass 1328.14m/z in the Y-ion series fragmentation of the MS^2 spectra exclude Ser209 and Ser205 at the phosphorylation site, however, there is insufficient MS^2 ion evidence (b1–9) to pinpoint the phosphorylation site specifically to Ser197 or Ser201, thus both sites with an * are potential sites of phosphorylation. Note: peptide is displayed C- to N-terminus due to the predominant Y-ion fragmentation.

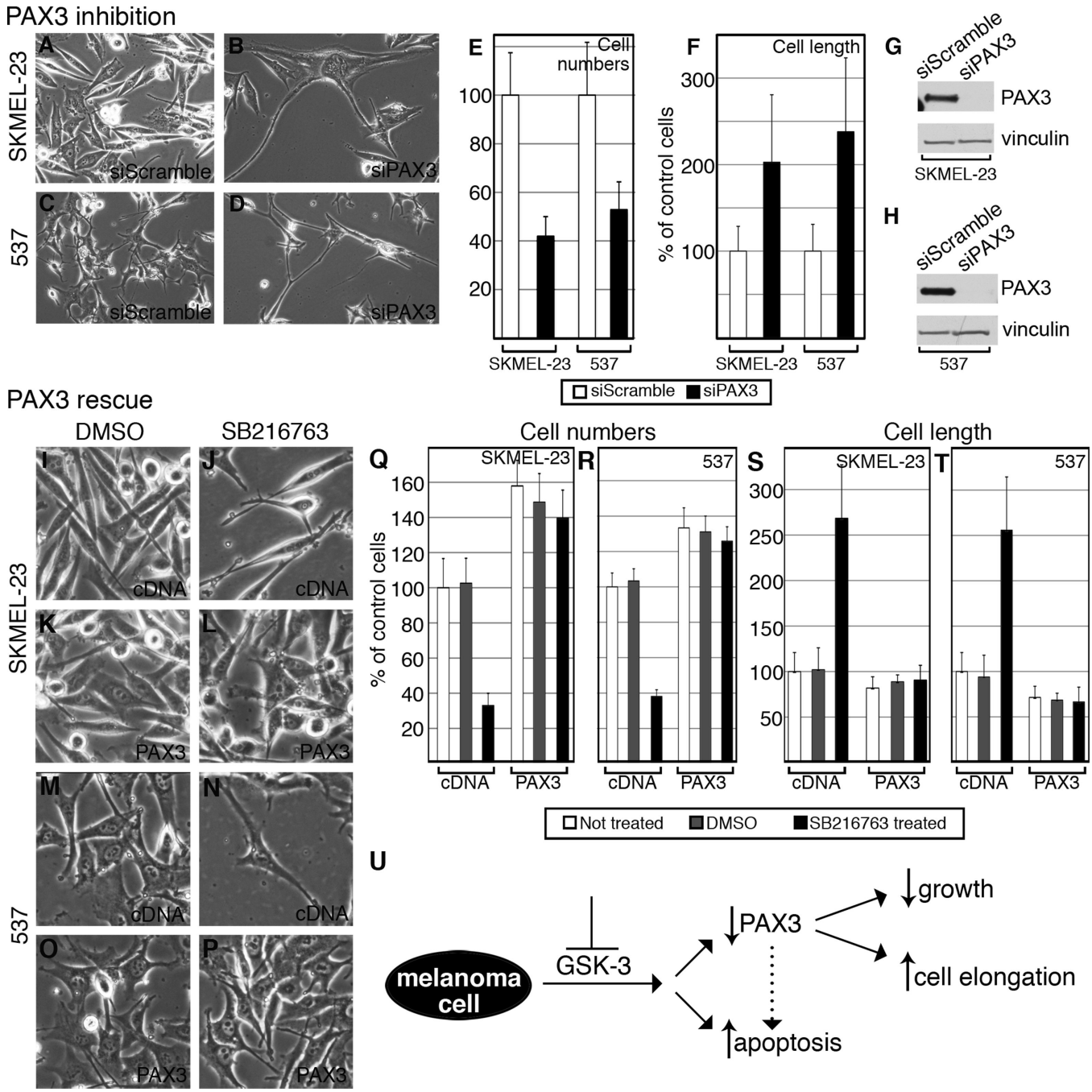

Figure 7.

PAX3 knockdown replicates cell phenotypes of GSK-3 inhibition (A–H) and PAX3 over-expression rescues these phenotypes (I–T). A–D, overall morphology of SKMEL-23 (A–B) and 537 (C–D) transfected with siScramble or si*PAX3*. Cells transfected with si*PAX3* exhibited cell number reduction compared to siScramble at 72 hours. E, quantification of cell number reduction with si*PAX3*. Cells transfected with si*PAX3* were counted 72 hours post-transfection and compared to siScramble (set at 100%). Values are means +/− s.d. (n=600 cells). F, quantification of cell length upon transfection with siScramble or si*PAX3*. 10 cells were measured from 6 groups. The siScramble was expressed as a percentage of the control group (average set at 100%). Values are means +/− s.d. (n=60 cells). G–H, si*PAX3*

reduces PAX3 levels in total cell lysate of SKMEL-23 (G) and 537 (H) compared to siScramble. Blots were probed with PAX3 antibody and vinculin as a loading control. I–P, SKMEL-23 (I–L) and 537 (M–P) cells were transfected with pcDNA3 (I–J, M–N) or pcDNA3-PAX3-HA (K–L, O–P) and treated with DMSO (I,K,M,O) or SB216763 (J,L,N,P) for 72 hours and observed for cell population and overall morphology. Q–R, quantification of cell numbers in I–P. SKMEL-23 and 537 cells transfected with either pcDNA3 or pcDNA3-PAX3-HA were left untreated, treated with DMSO, or with SB216763 for 72 hours and counted and compared to the non-treated control (set at 100%). Values are means +/− s.d. (n=600). S–T, quantification of cell length from I–P. For each treatment, 10 cells were measured from 6 groups. The DMSO- and SB216763-treated groups were expressed as a percentage of the untreated cells (average set at 100%). Values are means +/− s.d. (n=60). U, summary schematic of the response of melanoma cells to GSK-3 inhibition. A loss of GSK-3 activity resulted in an overall reduction of PAX3 levels, a decrease in cell growth and survival, and cellular morphology changes in some but not all of the cell lines tested. While the effects on cell growth and elongation are linked to a loss of PAX3 in this study, this correlation could not be established between PAX3 loss and apoptotic induction. PAX3-dependent apoptosis has been reported in melanoma cells, however, and is indicated with a dotted arrow (20, 24).